CENTRIFUGAL PUMP PERFORMANCE: NUMERICAL SIMULATION AND EXPERIMENTAL DATA COMPARISONS

Willian Segala, wsegala@gmail.com
Rigoberto E. M. Morales, rmorales@utfpr.edu.br
PPGEM/UTFPR, Av. Sete de Setembro 3165, CEP. 80230-901, Curitiba-PR-Brazil

Fernando A. França, ffranca@fem.unicamp.br
DEP/FEM/UNICAMP, Cid. Universitária s/n, Barão Geraldo, Cx. P. 6122, CEP. 13083-970, Campinas-SP-Brazil

Sergio C. Vincent, schiva@emc.uji.es
Nestor Ramos García, nrg@mek.dtu.dk
Universidad Jaume I, Av. de Vicent Sos Baynat s/n 12071, Castellón de la Plana - Spain

Abstract: *Centrifugal pumps are among the most used equipment in industrial plants. Besides that, efforts to infer the so-called pump performance curves are still required, mainly when the pump is used to transfer fluids that have a history of properties change, as the viscosity or density and chemical composition. This is a quite common situation in the oil industry, when electrical submersible pumps,* aka *ESPs, are used as the artificial lift method for oil production. The fluid properties change during the reservoir depletion period: the lighter and less viscous oil appears first, at this stage the gas-oil rate – GOR - is frequently the highest, water usually shows up during production, either naturally or caused by artificial injection, at an increasing content - BSW, emulsions may be formed and so on. As such, the oil production is a non-stationary process that poses difficulties for the pump proper selection and performance estimation. The result is that along the pump life time the operator has to rely on empirical correction charts to find the so-called de-rating factors and then to predict the performance trends. Computer fluid dynamics - CFD – modeling may become a reasonable alternative as soon they can produce reliable results for a variety of fluid properties in short time at adequate costs. Focusing on these aspects this paper presents the preliminary CFD results on the operation of a centrifugal pumps delivering water. This pump is similar to a radial ESP commonly used in oil wells (Lazarkiewicz similariyt criterion, for a low flow rate in-well pump -DN-280 model, radial impeller, N_q = 8 rpm at BEP or N_s = 1000, when $N \equiv min^{-1}$; $Q \equiv gpm$; $H \equiv ft$, flow rate and head taken from the water baseline curve). The simulation was performed for the set conservation equations written in terms of generalized coordinates, the rotor was set on a non-inertial system with the centrifugal force field imposed as source terms. The connection between the impeller and the diffuser is made through sliding grids. The turbulence model $k-\varepsilon$ was used. Experimental data were used for model validation. In future researches the simulation and the experimental validation will be extended for viscous fluids in the range of 100 cP to 1000 cP.*

Keywords: *Centrifugal pump performance, CFD, pump performance experimental tests, sliding grids.*

1. INTRODUTION

Centrifugal pumps are widely used equipment in chemical and power plants, in water distribution systems, in oil production and transportation facilities and many other areas. The proper selection of a pump assures a long operation time between failures (MTBF) and increases the pumping system effectiveness in terms of energy consumption and control. Nevertheless, the pump selection, including the operational performance sizing, still relies on experimental calibration data and correction factors to adjust the baseline curves to actual operation, according to the fluid properties. There are various difficulties to generate precise mathematical simulations of the pump performance curves. The flow in a pump is intrinsically short term transient (mili-second periods) and long term nonstationary (weeks, month or even a year), depending on the phenomenon under consideration. Very short transients take place, from 1 ms to 10 ms for instance, when the upflow in static channels interact with the displacing surfaces in rotating channels, or vice-versa. These occur at the rotor and diffuser entrances and impose fluid instabilities that have to be accounted for the proper pump performance modeling. Added-up to the flow recirculations caused by the non-tangential impinging flow, these combined processes create the so-called acceleration or de-acceleration "shocks", or viscous dissipation, at these locations. Local dissipation at channel entrances and the regular viscous dissipation in channel flows are the main causes for the energy loss inside pumps.

Nonstationary long term changes (the statistics of the process evolve with time) may arise when the system characteristics vary, the pump itself degrades (increasing clearances, for instance) or the fluid properties change. These are quite usual in oil production as the reservoir pressure may reduce during the depletion period. The pumps work in very harsh environments, under extreme operational conditions and the displaced mixtures have a long term history of property changes. Besides these, other processes, like cavitation, have to be predicted as they impose limits for the pump operation.

The pump performance is set by the relationship between the head, efficiency or power *vs.* flow rate, having the pump speed, fluid density and viscosity as parameters. The pump selection requires, among other technical data, the knowledge of its baseline performance curves obtained with a reference fluid, usually water, and the long term changes in the pump system characteristics and fluid properties. To correct for fluid properties variations, the most used approach was set by the Hydraulics Institute - HI, USA (1983). The empirical HI *abacus* provides de-rating (or correction) factors for flow rate, head and efficiency according the fluid properties, density and viscosity, having the baseline operational conditions as references. The de-rating factors are rough estimations as they were neither obtained for various types of centrifugal pumps not for an extended range of fluid properties. On this subject refer to Amaral *et al.* (2008). When the MTBF is a central criterion and the performance sizing with de-rating factors may be faulty, is becoming quite frequent to test ESPs – electrical submersible pumps used in oil production – with actual fluids when they are devised for critical applications in offshore and even onshore systems. If the pump performance could be reliably predicted by mathematical modeling and numerical procedures, using CFD – computational fluid dynamics, for instances, testing time would be saved and more detailed performance predictions would be delivered.

Many works have been done to assess the centrifugal pump performance and the flow characteristics under different operational conditions using CFD. More recently, Asuaje *et al.* (2004) focused on simulating the influence of a volute diffuser on the pressure and velocity fields inside a centrifugal pump impeller. Ridha and Nizar (2005) performed numerical simulations of the flow in pump impellers and diffusers using a sequential approach: the flow and pressure fields were first calculated in the rotating impeller. Then, the resulting velocity field obtained at the impeller exit were set as boundary conditions at the fixed diffuser inlet section. They have mentioned good agreement with experimental data besides the approach, clearly, did not account for the impeller blades passage across the diffuser entrance channel. Feng *et al.* (2006), also using CFD, found that a cross-dependence between impeller and diffuser channel flows exists. Recently, Amaral (2007) have disclosed that strong interactions exist between the impeller and diffuser channel flows at off-design conditions. Moreover, they also showed that the relative local viscous dissipation in regard with the pump head at the channels inlet section depended on fluid viscosity. Cheah *et al.* (2007) confirmed these experimental findings performing CFD calculations on the pressure and velocity fields in a commercial pump on design and off-design flow conditions. They have found that on the design condition limited recirculations took place at channel entrances, which produced the smoothest velocity distribution along the channels. As a result, the pump operation on the design point caused the lowest relative local dissipation. Conversely, the operation on off-design conditions set strong recirculations and local dissipation – "shock" - at the channel entrances: thus, reflecting on the pump overall performance.

To account for the interactions between rotating and fixed channels, an adequate approach might consider the simultaneous solution of the impeller and diffuser flows. The main difficulty arises when the flow variables calculated in the rotating grid (impeller) is to be transferred to fixed grid (diffuser). In this case, numerical simulation using multi-block domains (one rotating domain and one fixed domain) could be applied. To the common interface linking both domains - the sliding grid – has the function of transfer information between the two blocks. Experimental data are very important in such a development to calibrate and validate the numerical method itself, as well as to assess additional state-of-the-art processes, as the turbulence modeling and the turbulence suppression caused by a strong centrifugal field.

In this work the flow inside the impeller and the diffuser of a commercial centrifugal pump (model Imbil ITA 65-330/2, N_q = 8 rpm at BEP or N_s = 1000, where N ≡ min^{-1}; Q ≡ gpm; H ≡ ft, flow rate and head taken from the water baseline curve) is simultaneously solved using the multi-block sliding-grid implementation. The mass and momentum equations for water flows were solved using the finite volume technique and the standard SIMPLEC algorithm. The numerical data were compared with detailed experimental data taken in a loop setup prepared to operate with light and heavy – or more viscous – liquids, up to 1200 cP. As such, the present work is a first step of a longer journey devised for comparing detailed experimental data on the flow and pressure field inside centrifugal pumps, focusing on ESPs, and CFD calculated data. The aim is to verify the CFD techniques that are the most able to calculate the overall pump performance. A cooperation program involving two groups performing the numerical simulations – based at UTFPR, Brazil and Universidad Jaume I, Spain – and a group based at the LabPetro /Unicamp, Brazil, which produced the experimental results, was set.

2. THE EXPERIMENTAL SETUP

The setup used to test the Imbil ITA 65-330/2 centrifugal pump is depicted in Fig. 1. To allow for a full range test a series-connected booster pump was added to the system. As part of this set-up there were also two tanks for fluid storage (water and glycerine), a 40 kW heat pump for temperature conditioning between 10 and 70 ^{o}C, a compatible heat exchanger, a Coriolis flow meter, pipe accessories, various pressure and temperature sensors, a tork and speed sensor, frequency inverters, a data acquisition system and a computer. The tested and the booster pump were connected in a series arrangement to make possible pressure adjustments at the tested pump intake to avoid cavitation and to extend the tests over the full flow range between the shut-off up to the non-head condition. The heat pump and the heat exchanger included in the set-up conditioned the fluid temperature to ensure constant properties and allow tests using clear glycerine in the range of 60 cP to 1200 cP, besides the tests performed with water. The frequency inverter drives allow the booster and tested pump speed regulations and fine adjustments in test conditions, pressure and flow rates in various pump speed. The experimental apparatus is also prepared to test ESPs – multistage centrifugal pump used for

artificial lift in oil wells. For this kind of pumps, a test skid with additional instrumentation, frequency inverter and a 50 HP motor is also part of this system, in a series parallel arrangement. The set-up is at LabPetro/Unicamp.

The conventional centrifugal pump simulated and tested for this work is a two stages unit, closed impeller type with eight backward curved blades, twelve vanes diffuser mounted just after the first impeller, an eight vanes inducer and a volute connecting the second impeller to the pump outlet. The pump inlet eye is 75 mm ID and the pump discharge pipe is 62 mm ID. The first impeller main dimensions are 80.0mm ID and 205.0mm OD; the vane intake angle, β_1, is 22.5°; the vane exit angle, β_2, is 36°; the first impeller channel width, δ_1, is 21.0mm at the intake and 12.0mm at the exit section, δ_2. The second impeller dimensions are 76.0mm ID and 260.0mm OD; $\beta_1 = 23.5°$, $\beta_2 = 36°$, $\delta_1 = 21.0$mm and $\delta_2 = 8.0$mm. The ITA 65-330/2 pump was first tested with its original steel inlet cover; afterwards, the Plexiglas cover replaced it to make fast speed flow visualization possible.

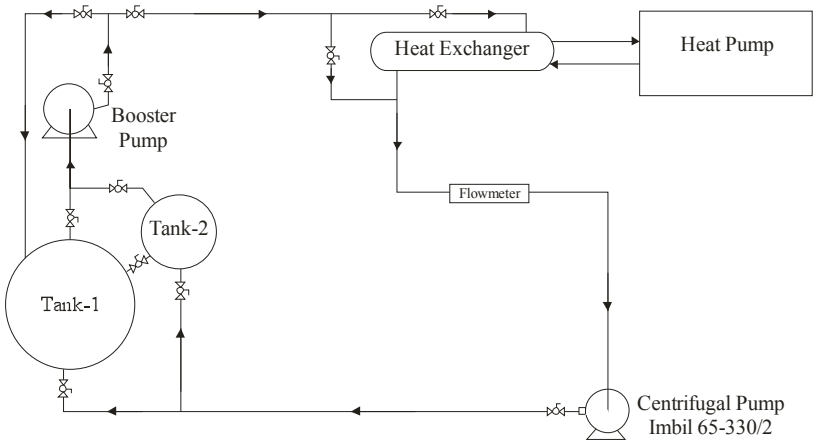

Figure 1 – Schematics of the set-up for testing conventional and ESP pumps

In Fig. 2 there are pictures showing details of the pump set-up, connection taps and instrumentation. In Fig. 2(a) appears the vertical mounted pump with its original suction cover and the set of capacitance pressure transducers (upper left) used to measure the pressure evolution along the pump channels, from the inlet eye to discharge section. Figure 2(b) shows the Plexiglas suction cover used during the experimentations to allow for the flow visualization.

Figure 3(a) shows the schematics of the pump radial internal view, where appears, according to the flow direction, the suction cover, the first impeller, the diffuser-inducer set, the second impeller and the volute diffuser that finishes at the discharge section. The tests with the original iron cover were followed by tests with the Plexiglas cover to have the baseline performance curves (head, power and efficiency vs. water flow rate), having the impeller speed as a parameter. Detailed measurements of the pressure evolution along the channels were performed to calculate the viscous dissipation in the pump main components (impellers, diffuser-inducer, second impeller and volute) and to estimate their contribution in terms of the energy transfer and dissipation. In Fig. 3(a) the numbers inside circles indicate the six internal positions where the pressure was measured. For instance, subtracting the pressure measured at 1 from the pressure measured at 2, the pressure gain across the first impeller is obtained; from 2 and 3 the pressure difference across the diffuser is found, and so forth.

(a) (b)

Figure 2 – (a) Vertical-mounted Imbil ITA 65-330/2 with motor, tork sensor, pressure sensors (upper-left) and frequency inverters (background); (b) details of the Pexiglas intake cover and pressure taps.

In Fig. 3(b) the schematics represents the first stage set, formed by the impeller and the radial outwards diffuser. At the diffuser outer limit a singularity exists, as the flow to undergo a section restriction before entering the radial inward inducer. More details on this region will be presented latter on.

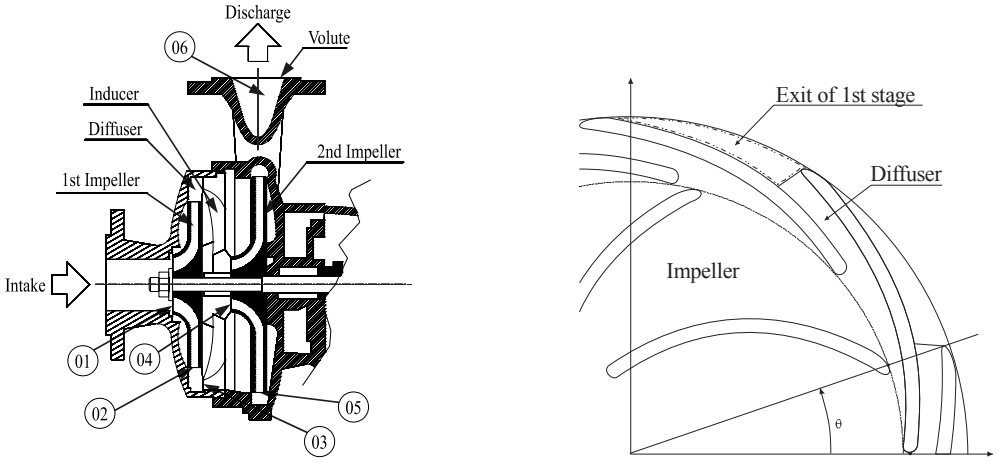

a) (b)

Figure 3 – (a) ITA 65-330/2 internal parts and pressure measurement locations (circled numbers), radial plane view; (b) schematics of the pump first stage, front plane view.

3. MATHEMATICAL MODEL AND NUMERICAL TECHNIQUE

In this section the most relevant assumptions and the mathematical model used for the numerical calculations are presented. The first stage numerical domain, as implemented in the CFX 11.0 CFD package, is showed in Fig. (4). Numerical simulation were performed for flow rates within the 10 to 50m^3/h flow range, for various pump speed, 1150rpm, 1000rpm, 806rpm and 612rpm. The working fluid used in these first calculations was tap water at constant 25°C: density $\rho = 997.0\ kg/m^3$ and dynamic viscosity $\mu = 8.9.10^{-4}\ Pa.s$. The mass and momentum conservation equations for a Newtonian fluid in transient, incompressible and isothermal flow can be written in a generalizing form as

$$\frac{\partial}{\partial t}(\rho\phi) + \nabla.(\rho\vec{V}\phi) = \nabla.(\Gamma_\phi \nabla\phi) + S_\phi + P_\phi \qquad (1)$$

where t is the time, $\vec{V}$ is the total velocity vector, ρ is the fluid density, $\phi = 1$ and $\Gamma_\phi \equiv S_\phi \equiv P_\phi \equiv 0$ represents the mass conservation and $\phi = \vec{V}$, $\Gamma_\phi = \mu_{eff}$ (effective dynamic viscosity) and S_ϕ and P_ϕ are source terms when the momentum equation is considered. The term S_ϕ may become a combination of superposed effects like the Coriolis and the centrifugal force fields and P_ϕ represents the pressure gradient exerted on a fluid unit volume, usually written as ∇P. Depending on fluid properties and operational conditions, as in water transport, the channel flows are turbulent and the effective dynamic viscosity must account for it. The $\kappa - \varepsilon$ turbulence model (Launder and Spalding, 1974) was used for this purpose.

The set of differential partial equations in a discrete form was used by the CFD package ANSYS CFX 11.0 to calculate, using the finite volume approach, the velocity and pressure fields for a prescribed three-dimensional domain. This domain was formed by several non-regular control volumes resulting a non-structured mesh. CFX uses the SIMPLEC algorithm to solve the coupling pressure-velocity problem (Van Doorman and Raithby, 1984), with co-located mesh and hybrid scheme to interpolate the convective terms. All the numerical simulation were performed using Intel Pentium IV, Dual Core 2, 64 bits in a computer and, also, in Racks Fujitsu Siemens with two parallel CPU cores.

The numerical domain calculation encompassing the stage was divided in three sub-domains: pipe intake, first impeller and diffuser. Figure 4(a) shows the geometric model used in the numerical simulations. In Fig. 4(b), the three sub-domains used by the CFX package are disclosed. The pipe intake domain is a small static cylinder, with 85.0mm ID and 50.0mm long. The first impeller geometry was modeled and the mesh was generated for this geometrical model. The entire impeller domain rotates with a constant speed. At the pipe intake-rotor interface an "*interface model general connection*" boundary condition was applied. It transfers information from the stationary domain to the rotating one, and vice-versa. The diffuser was modeled in a similar way as the impeller. The "*interface model general connection*" boundary condition set the transition from the impeller outlet to the diffuser as well. A mesh test was done and the optimum configuration used in the simulation was formed by 4532 nodes in the pipe intake, 152011 nodes in the impeller and 200835 in the diffuser.

To account for the interacting transient process taking place when the flow leaves the rotating impeller and enters the stationary diffuser having blades at pre-defined angular positions, it is necessary to establish a relative reference position for both impeller and diffuser. Doing so, the angle θ is defined and measured from a certain diffuser blade and sets this relative reference frame, as shown in Fig. 3(b).

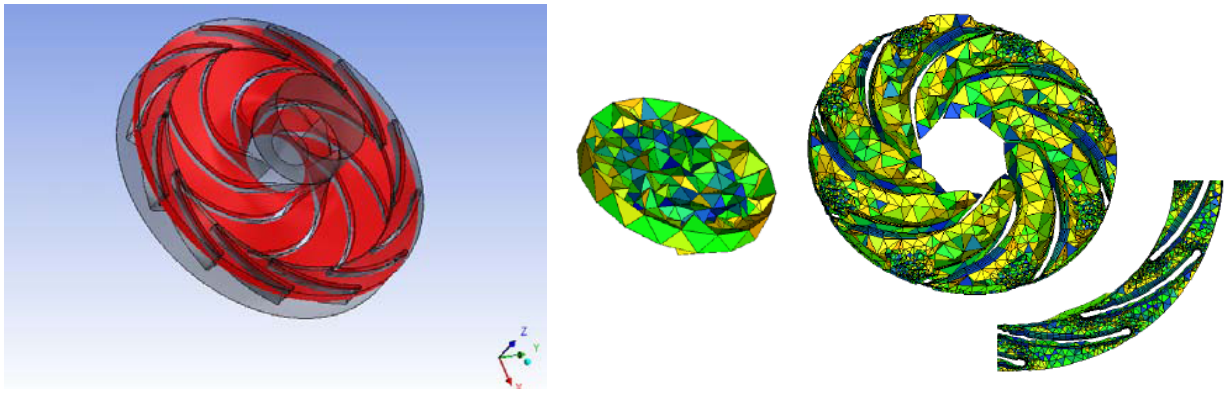

(a) (b)

Figure 4 – (a) Numerical domain used in software CFX; (b) Non-structured mesh for Imbil 65-330/2 pump simulation at: intake pipe, impeller and diffuser.

4. RESULTS

In this section the numerical results and their comparisons with the experimental ones are presented and discussed. The first procedure was to model the flow through a stationary pump first stage (non-rotating impeller). The objectives were two-fold: to verify the proper setting of interfaces between domains and to generate a view of streamlines inside the entire flow domain. Figure 5 shows one of these set of calculated flow lines at the solid frontiers of the physical domain.

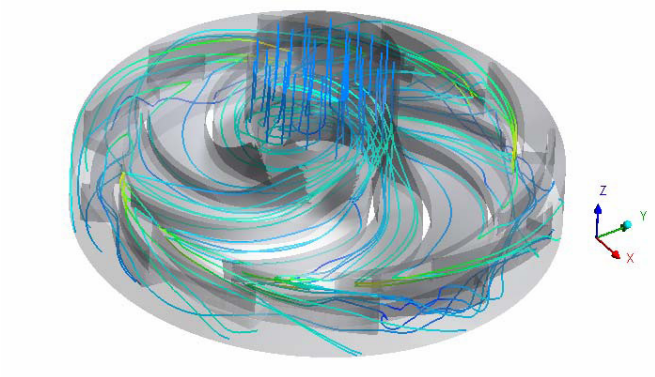

Figure 5 – Flow through a stationary pump first stage. (non-rotating impeller). Visualization of flow lines from intake pipe to diffuser exit.

Figure 6 shows the calculated pressure and relative velocity – concerning the impeller - oscillations at the rotating impeller-diffuser boundary as a function of θ, the relative impeller-diffuser angular position, at a fixed time. The fast coupling between velocity and pressure appears clearly, the pressure increase is always connected to a velocity decrease, and vice-versa. The full squares at the bottom side of Fig. 6 represent the position of the diffuser blades and the full circles at the top represent the impeller blade presence. The oscillation is periodic in regard with the angular position, repeating every 90° angular displacement.

Figure 7 discloses the relative velocity oscillations as a function of θ in four different instants at the impeller-diffuser boundary. It is important to notice that fluid relative velocity reaches minimum in front of the diffuser blade, as it should be: when the fluid leaves the impeller, it has a solid surface in front of it, causing de-acceleration and pressure increase. The simulation was performed for various pump (impeller) speeds and the flow rate was used as a calculation parameter for comparisons. The experimental data on the pump overall perforce and pressure differences across impeller and diffuser, taken for these very same speed, were used for comparisons.

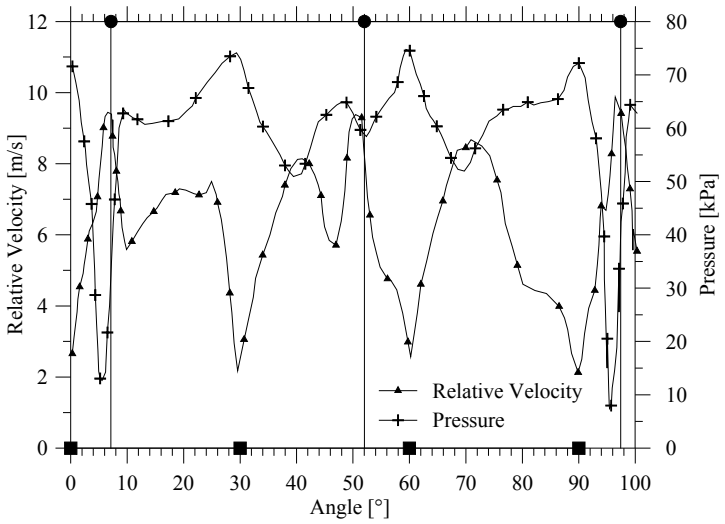

Figure 6 – Pressure and relative velocity at the impeller-diffuser boundary as a fuction of θ. (The flow rate is 30m^3/h and the rotation used is 1150 rpm)

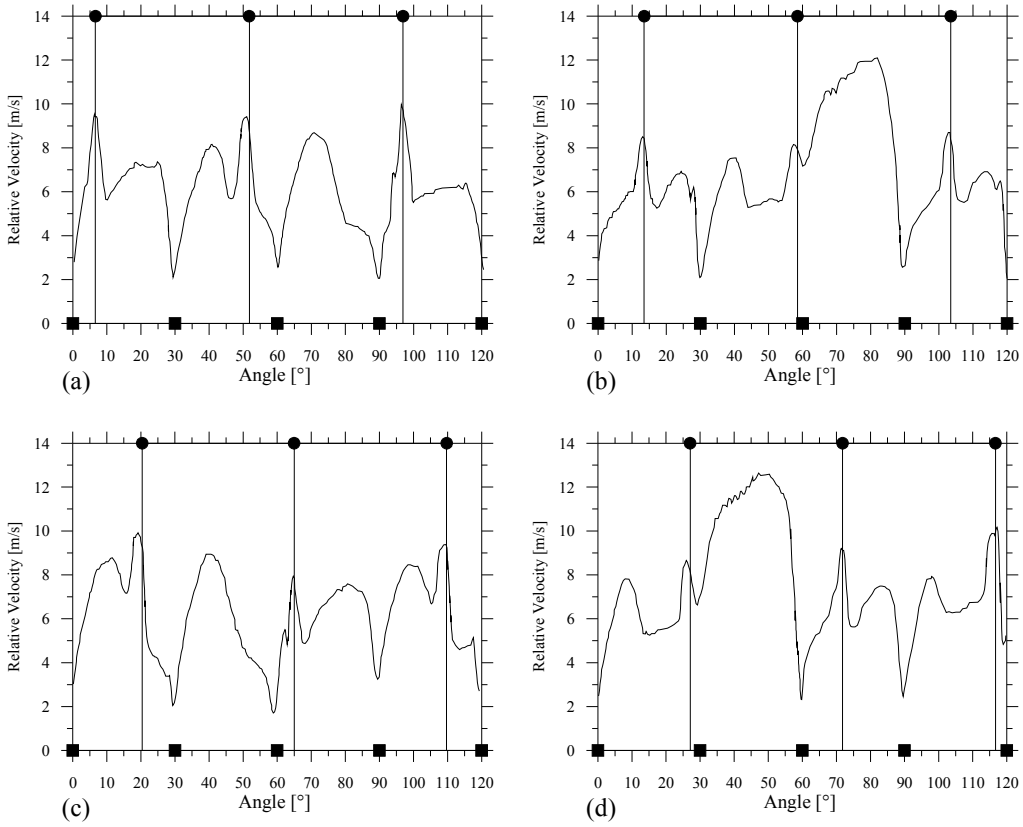

Figure 7 – Relative flow velocity at the impeller-diffuser boundary as a function of θ in four time steps. (The flow rate is 30m^3/h and the rotation used is 1150 rpm)

The pump performance, in terms of head vs. flow rate can be obtained summing up the pressure difference across impeller and diffuser for a given speed. In a multi-stage ESP pump, for instance, the total head for a given flow rate is easily obtained multiplying the unit head by the total number of stages. The comparisons between impeller and diffuser partial contributions for the unit or total head, numerical and experimental data, give rises to the appropriateness of the mathematical simulation in these singular components. These comparisons, for the pressure difference data across the first impeller, appear in Fig. 8 for various pump speed. The agreement between them can be stated as very good, as the average deviation was +8% in favor of the measured data. The highest deviations appear to happen at the highest flow rates, indicating that the viscous dissipation could be slightly over predicted under this condition. Some turbulence intensity suppression due to the strong centrifugal fields and curvature effects on the flow field and turbulence models could be argued to explain these deviations.

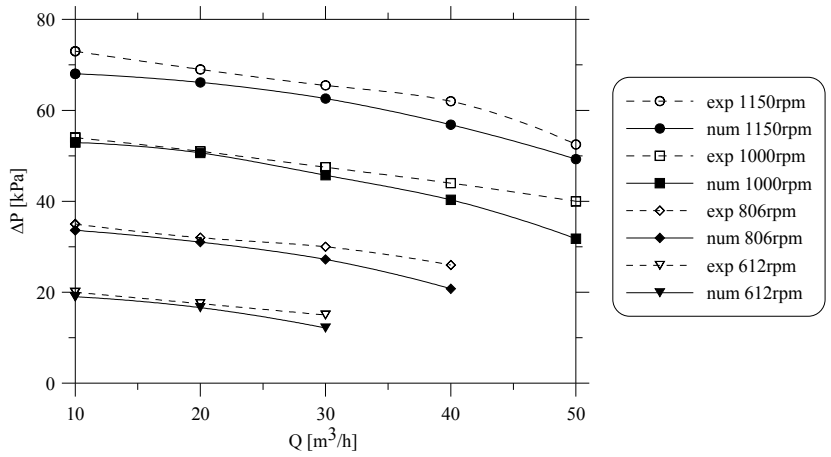

Figure 8 – Pressure difference across first impeller, Imbil 65-330/2 water operation: comparisons between numerical and experimental data.

The pressure variation across the diffuser is shown in Fig. 9. The deviations between numerical and experimental data were relatively higher for the diffuser than for the impeller. A wrong pressure boundary condition imposed at the diffuser exit section could be argued as an error source. Just after the fluid leaves the diffuser it has to flow through a singularity that imposes both a sudden section restriction and a radial outwards to a radial inwards direction change - refer to Fig. 3(b). As such, the pressure boundary condition at the diffuser exit section is not trivial and its actual influence on flow field may not be properly represented in the present simulation. There are, also, controversies on the experimental data, as the pressure tap location at the diffuser exit may suggest that the data is not purely a static pressure one. In this sense, a velocity component would increase the actual static pressure difference.

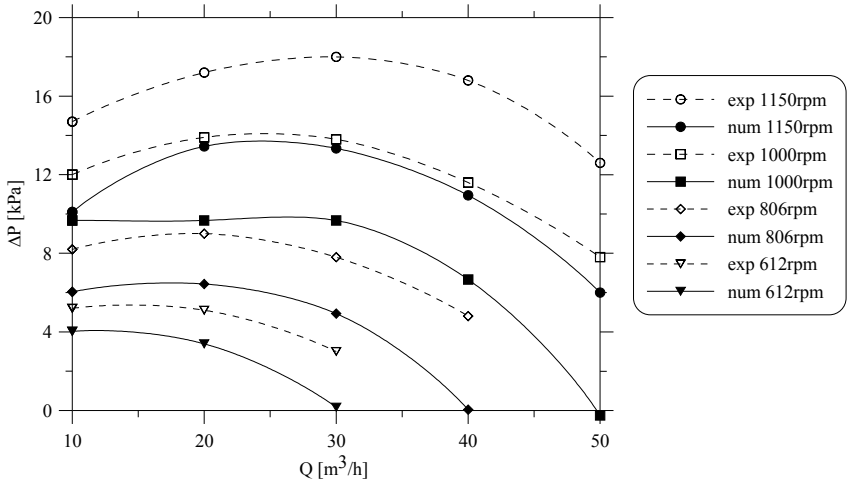

Figure 9 – Imbil 65-330/2 pressure difference across the diffuser vs. flow rate, numerical vs. experimental data for various pump speed.

Adding up the impeller and diffuser pressure difference for a fixed flow rate, the pump stage performance in terms of pressure difference or the pump head vs flow rate is obtained, Fig 10. As expected, the diffuser data deviations propagate for the total pressure calculations. However, as the diffuser is less responsible for the pressure gain -in the highest flow rate ranges, above the BEP condition, even energy dissipation was measured – the total pressure calculated and experimental data deviations tend to be acceptable.

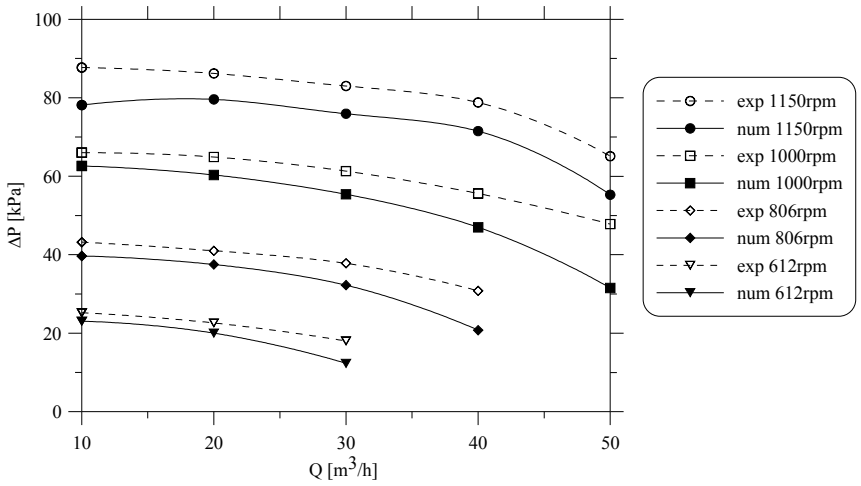

Figure 10 – Imbil 65-330/2 first stage performance curve, pressure difference vs. flow rate, numerical vs. experimental data for various pump speed.

5. CONCLUSIONS

The results obtained in the numerical simulation have reached good agreement with the experimental data. The deviation in the results in the first pump stage is about 10%. Nevertheless, several points must be considered. There are evidences that due to the presence of a strong centrifugal field in the flow, turbulence suppression could take place, mainly for high values of flow rate. Thus, the used turbulence model could be over estimating the viscous dissipation inside the impeller and diffuser. The singularity located on the diffuser exit, was not correctly modeled and, consequently, its effects on the flow were not captured. This could explain the deviation between the experimental and numerical data.

The sensor where the pressure in the diffuser exit is measured probably is not correctly located. It´s possible that the pressure obtained at this point was not completely static. This could bring the diffuser curves closer (numerical and experimental).

It is necessary to evaluate a better turbulence model able to capture effects comes from rotating bodies and curveted walls as well. With these recommendations it´s expected that the agreement between numerical and experimental data numerical ones improves itself.

6. REFERENCES

ANSYS CFX Release 11.0. *"ANSYS CFX-Solver Modeling Guide"*, December 2006.

Amaral, G., Estevam, V. and Franca, F. A., 2008, "*On the Influence of Viscosity upon ESP Performance, SPE Production and Operations*" (in press).

Asuaje, M, Farid, B, Kouidri, S., Kenyery, F. and Rey, R., 2005, "*Numerical Modelization of the Flow in Centrifugal Pump: Volute Influence in Velocity and Pressure Fields*", International Journal of Rotating Machinery, Paris, France, pp. 244-255.

Cheah, K.W., Lee T.S., Winoto, S.H. and Zhao, Z.M., 2007, "*Numerical Flow Simulation in a Centrifugal Pump at Design and Off-Design Conditions*", International Journal of Rotating Machinery, Singapore, 8 p.

Feng, J, Benra, F.K. and Dohmen, H.J., 2007, "*Numerical Investigation on Pressure Fluctuations for Different Configurations of Vaned Diffuser Pumps"*, International Journal of Rotating Machinery, Duisburg, Germany, 10 p.

García, N. R. and Vicent, S. C., 2007 "*Simulacion, análisis y rediseño de bombas centrífugas*", 315p. Castellon de la Plana, Spain, Industrial Engineering (Degree).

Hydraulic Institute – USA, 1983, "*Hydraulic Institute Standards for Centrifugal, Rotary & Reciprocating Pumps,*" 14th Edition.

Launder, B. E. and Spalding, D. B. *"The Numerical Computation of Turbulent Flows"*, Comput. Methods Appl. Mech. Eng., vol. 3, pp. 269-289, 1974.

Patankar, S.V. *"Numerical Heat Transfer and Fluid Flow".* Hemisphere Publishing Corp, 1980.

Ridha, Z. and Souissi, N.B., 2005, "Predicting Appearance of Cavitation in Pumps with a Numerical Approach"

Van Doormal, J. P. and Raithby, G. D. "*Enhancements of the SIMPLE Method for Predicting Imcompressible Fluids Flows*", Numerical Heat Transfer, Vol. 7, pp. 147-163. (1984)

7. RESPONSIBILITY NOTICE

The author(s) is (are) the only responsible for the printed material included in this paper.